Applied Biological Research 24(4): 429-439; (2022)
DOI: 10.5958/0974-4517.2022.00051.9

In silico ANALYSIS OF NOVEL ANTICANCER AGENTS AS BRD4 INHIBITORS

Vindhya Vikram Singh* and Shafqat Alauddin

Cheminformatics and Molecular Modelling Lab, Department of Chemistry,
Shibli National College, Azamgarh – 276 001, Uttar Pradesh (India)
*e-mail: *vindhyavikrams@gmail.com*

(Received 27 April, 2022; accepted 18 October, 2022)

ABSTRACT

The BET BRD4 proteins, involved in cancer, are of prime importance in developing anticancer drugs. Cancer is marked by the uncontrolled growth of abnormal cells anywhere in the body with the potential to spread or invade other body parts. The core nature of disease lies in defying normal cell signals, be it anti-growth signals, death signals or apoptosis, and tissue invasion metastasis. In present work, we have designed and tested novel quinazolinone-based derivatives to establish them as a better anticancer agent against the BRD4 target. The selection of BRD4 protein in this work is based on earlier findings that reported the role of BRD4 in various cancers such as lymphoma, multiple myeloma, acute myeloid leukemia, acute lymphoblastic leukemia, chronic myeloid leukemia, solid tumours, prostate cancer, nervous system tumour, colorectal cancer, and breast cancer. Molecular docking was performed by using Glide docking module of the Schrodinger suite. The XP Glide docking studies, ADME (absorption, distribution, metabolism, excretion) profile test, binding energy calculations, and drug-likeness was performed to get the best BRD4 inhibitor ligand. Out of 16 quinazolinone derivates, ten ligands had better XP Glide score, 4 were marginally less, and 2 gave poor score than the standard drug LY2 (-6.779 kcal mol^{-1}). The best ligand had a score of -9.866 kcal mol^{-1} which was 45% more efficient than LY2, so appears to be more effective and potent anticancer inhibitor ligands for BRD4 protein.

Keywords: Anticancer drugs, BET BRD4 proteins, molecular docking, protein inhibition, quinazolinone derivatives, targeted therapy

INTRODUCTION

Cancer is the most dreadful disease in human societies around the globe owing to its very complex nature and high mortality rate. The situation is worse in poor and developing countries due to the lack of basic medical facilities and improper treatment (Bray *et al.*, 2018). There are around 200 types of cancer, and among them the top five cancers account for 47.2% cancers (Saranath and Khanna, 2014). These cancers can be cured if detected early in the survivors. As per WHO report, a total of 19.3 million cancer cases have been reported around the world and in 2020, around 10 million deaths were reported from cancer disease alone (Sung *et al.*, 2021). Conservative estimates reveal that by 2030 there will be about 70% increase in mortality from cancer with worldwide estimate of 13.1 million deaths, and in India the prevalent cases of cancer within five years will be more than 2.7 million (Sung *et al.*, 2021).

Cancer means the uncontrolled growth of abnormal cells anywhere in the body with the potential to spread or invade other body parts. The core nature of disease lies in defying normal cell signals, be it anti-growth signals, death signals or apoptosis, and tissue invasion metastasis

(Hanahan and Weinberg, 2011). The traditional treatment methods for cancer include surgery, chemotherapy, and radiation. Surgery and radiations have limitations that in surgery the patients have to tolerate both surgery and anesthesia, and requires excellent precision during surgery because any diseased cell left will fail the whole treatment. Radiation and chemotherapy have disadvantage of damaging the surrounding non-diseased tissues and healthy cells (Crisci *et al.*, 2019). The advancement in treatment is called targeted therapy which is also referred to as the new generation of cancer treatment, which uses drugs or other substances to more precisely identify and attack cancer cells, usually with no or very little damage to normal cells (Gerber, 2008). Chemotherapy and targeted therapy both use drugs, but the fundamental difference between them is the cytotoxic nature of chemotherapy drugs as they can kill normal cells with cancer cells (Crisci *et al.*, 2019). Targeted therapy is branched into monoclonal antibodies and small molecule inhibitors. Small molecule inhibitors differ from monoclonal antibodies as they are orally administered and generated via a step-by-step chemical practice; this is often a very cost-effective method whereas monoclonal antibodies are infused via penetration into the patient's body and involve recombinant DNA techniques, a very costly method used in biotechnology. In present study, our approach was to identify small molecule inhibitors with potential against the BRD4 target. Currently, there are many therapeutic targets and their inhibitors which have been identified and used as a drug against the target while many are in the various stages of clinical trials (Crisci *et al.*, 2019; Pucci *et al.*, 2019). These molecules target cancer drugs have cured a large number of patients (Padma, 2015).

The proteins directly linked to the survival and progression of cancer are the ones to which cancer cells are addicted (Weinstein and Joe, 2008). Once the disease is rooted in the patient's body these proteins provide all the help needed in cancer development so these proteins can be targeted for inhibition and the inhibitor molecule will be the anticancer drug. In this work, we tried to find out novel inhibitors for Bromodomain and extra terminal (BET) BRD4 protein (Xu and Vakoc, 2017; Stathis and Bertoni, 2018; White *et al.*, 2019). The BET family of proteins was earlier identified as epigenetic regulators in inflammatory processes. Various researchers have established the role of BET proteins in reading chromatin and recruiting the chromatin regulating enzymes to control gene expression in many pathological processes and cancer (Donati *et al.*, 2018; Stathis and Bertoni, 2018; White *et al.*, 2019). The aim was to look after the relation of BRD4 proteins with cancer and their role in inhibition of BRD4 protein thereby in lessening the cancer development.

Quinazolinone ($C_8H_6N_2O$), a heterocyclic quinazoline ($C_8H_6N_2$) with a carbonyl group in C_4N_2 ring and a prominent pharmacophore, is regarded as a very potent and privileged structure in medicinal chemistry (Nagaraju, 2015; Ajani *et al.*, 2016). These structures have high affinity to bind at multiple sites so may be medicinally useful compounds. Quinazolines have broad spectrum biological properties like antibacterial, antifungal, anti-inflammatory, anticonvulsant, anti-HIV, analgesic, and anti-cancerous activities; and many quinazolinone-based drugs are available in the market (Subramaniam *et al.*, 2011; Tiwary *et al.*, 2015). Quinazolinone and its derivatives are building blocks for nearly 200 naturally occurring alkaloids isolated from several plants, microbes, and animals (Singh *et al.*, 2013; Tiwary *et al.*, 2015; Kavitha *et al.*, 2018). In present study we tested quinazolinone derivatives on BRD4 protein (PDB ID: 3MXF) for inhibition of BRD4 proteins to curb cancer so as to establish the anticancer nature of these ligands. To verify our results, we choose a well-known inhibitor of BRD4, an anticancer drug LY-294002 also known as LY2 (Drug bank ID: DB02656).

MATERIALS AND METHODS

Protein selection and preparation

BET (bromodomain and extra terminal) BRD4 protein (PDBID-3MXF) crystal structure having a resolution of 1.60Å was obtained from PDB database (*https://www.rcsb.org/3mxf*). This PDB

complex was prepared using the protein preparation wizard workflow of Schrodinger software suite (Madhavi Sastry *et al.*, 2013). Initially, all the bond orders in protein were assigned, hydrogen atoms added and all crystallographic water molecules removed. Subsequently, the missing residues and loops were filled using Prime module of Schrodinger 2017-2 (Jacobson *et al.*, 2004). The protein complex was subjected to energy minimization using OPLS3 force field with implicit solvation. The receptor grid was generated around the co-crystallized ligand of PDB complex (3MXF) at default parameters of Receptor Grid Generation tool of the Glide module (Friesner *et al.*, 2006).

Ligand preparation

Marvin tool was used for ligand design, Marvin version 18.18.0, ChemAxon. Further preparation of these designed ligands was performed using the LigPrep module of Maestro (Schrödinger release 2017-2 Maestro, Schrödinger, LLC, New York, USA). All the possible states were generated using the OPLS force field and all other parameters were kept as default.

Molecular docking

The ligand docking tool in the Glide module of Schrödinger Suite 2017-2 was used for docking studies. The Extra precision (XP) tool was used for accurate results and all the other settings were left to default (Friesner *et al.*, 2006).

Binding energy calculations

The molecular mechanics/generalized Born surface area (MM/GBSA) method was employed using the PRIME module of Schrodinger 2017-2 (version 11.2.013) (Jacobson *et al.*, 2004) for calculating the binding affinities of experimental ligands against BRD4. Prime/MM–GBSA method uses docked pose file of the receptor and ligand to calculate the binding free energy (ΔGbind) of each ligand in the workspace selected. The obtained ligand poses were minimized using local optimization feature in Prime, whereas the energies of the complex were calculated with OPLS3 force field and generalized Born/ surface area continuum solvent model.

ADME and drug-likeness prediction

ADME (absorption, distribution, metabolism, excretion) profiling was performed by Swiss ADME server of Swiss Institute of Bioinformatics (*http://www.swissadme.ch/)* (Daina *et al.*, 2017). ADME profile provides a quality assessment of the lead compounds. The chemical and drug-likeness properties of some top-scoring compounds were predicted to assess the suitability of these compounds as lead molecules. The methodology protocol used for the identification of potential inhibitors against BRD4 protein is as under:

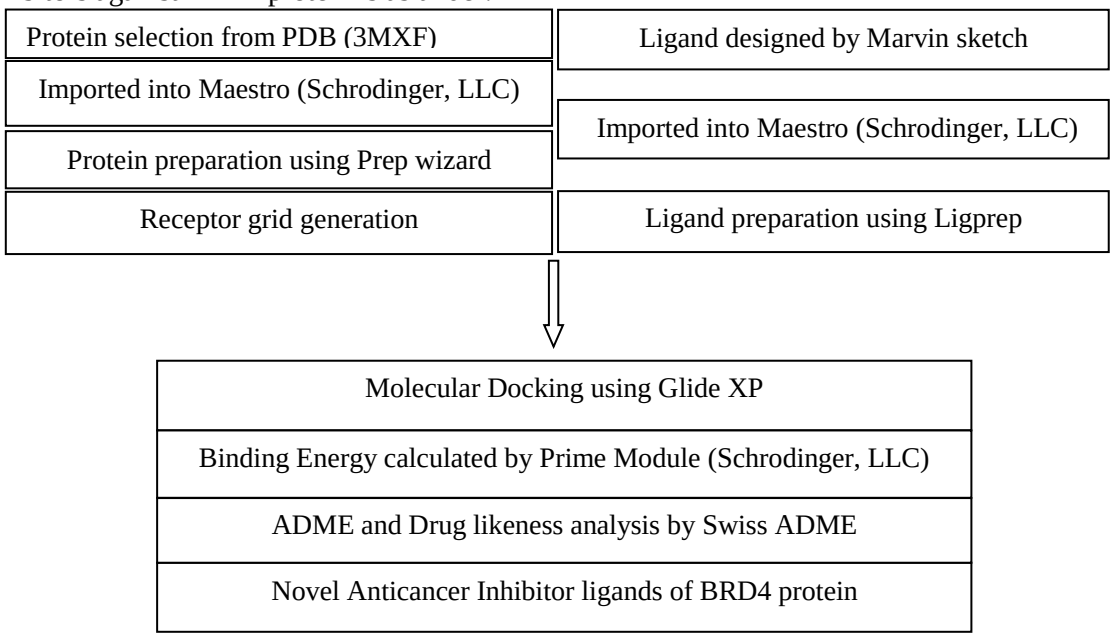

RESULTS AND DISCUSSION

The Glide docking study identified 5A, 5E, and 5C as the top three scoring compounds having docking scores of -9.866, -9.857, and -9.616 kcal mol^{-1}, respectively, which was greater than the standard drug LY2 (-6.779 kcal mol^{-1}) [Table 1]. Out of the total 16 designed ligands, 10 ligands had better scores, and 4 had marginally less score and only 2 ligands performed poorly than the standard drug (LY2). The other 7 compounds with higher glide dock scores than the standard drug LY2

Table 1: Interacting residues of BRD4 protein withLY2 and experimental ligands (3A to 5F) with their Glide Dock scores

Ligands	Glide dock score (kcal mol^{-1})	Interacting residues
LY2	-6.799	LEU92, LEU94, TYR97, TRP81, PRO82, PHE83, GLN85, VAL87, CYS136, TYR139, ASN140, and ILE 146
3A	-6.685	LEU 92, LEU 94, TYR 97, PRO 82, PHE 83, VAL87, MET132, ASN 135, ASN 140, CYS 136, TYR 139, and ILE146
3B	-6.830	LEU 92, LEU 94, TYR 97, TRP 81, PRO 82, PHE 83 VAL 87, MET105, ASP106, MET132, ASN 135, CYS136, TYR 139, ASN 140, and ILE146
3C	-6.190	LEU92, LEU94, TYR97, TRP81, PRO82, PHE83, GLN85, VAL87, ILE101, MET132, ASN135, CYS136, TYR139, ASN140, and ILE146
4A	-8.049	LEU92, LEU94, TYR97, TRP81, PRO82, PHE83, GLN85, VAL87, ASP88, MET132, ASN135, CYS136, TYR139, ASN140, ASP145, and ILE 146
4B	-7.620	LEU92, LEU94, TYR97, TRP81, PRO82, PHE83, GLN85, VAL87, MET105, MET132, ASN135, CYS136, TYR139, ASN140, and ILE146
4C	-5.741	LEU92, LEU94, TYR97, TRP81, PRO82, PHE83, GLN85, PRO86, VAL87, ASP88, CYS136, TYR139, ASN140, and ILE 146
4D	-6.610	LEU92, LEU94, TYR97, TRP81, PRO82, PHE83, VAL87, MET132, ASN135, CYS136, TYR139, ASN140, ASP145, MET149, and ILE 146
4E	-8.499	LEU92, LEU94, TYR97, TRP81, PRO82, PHE83, GLN85, PRO86, VAL87, ASP88, MET132, ASN135, CYS136, TYR139, ASN140, ASP145, and ILE146
4F	-7.425	LEU 92, LEU 94, TYR 97, TRP 81, PRO 82, PHE 83, GLN85, VAL 87, MET 105, ASP106, MET132, ASN135, CYS 136, TYR 139, ASN 140, ASP145, and ILE 146
4G	-4.267	LEU 92, LEU 94, TYR 97, TRP 81, PRO 82, PHE 83, VAL87, MET132, ASN135, CYS136, TYR, 139, ASN 140, ASP144, ASP145, ILE 146, and MET149
5A	-9.866	LEU 92, LEU 94, TYR 97, TRP 81, PRO 82, PHE 83, VAL87, ILE 101, MET132, ASN135, CYS 136, TYR, 139, ASN140 and ILE 146
5B	-6.740	LEU 92, LEU 94, TYR 97, TRP 81, PRO 82, PHE 83, VAL87, MET105, ASP106, MET132, ASN 135, CYS 136, TYR, 139, ASN 140, and ILE146
5C	-9.616	LEU 92, LEU 94, TYR 97, TRP 81, PRO 82, PHE 83, VAL87, MET132, ASN 135, CYS136, TYR, 139, ASN 140, and ILE146
5D	-7.361	LEU 92, LEU 94, TYR 97, TRP81, PRO82, PHE 83, VAL 87, MET105, MET132, ASN135, CYS 136, TYR139, ASN140, and ILE 146
5E	-9.857	LEU92, LEU94, TYR 97, TRP81, PRO82, PHE83, VAL87, ILE101, MET132, ASN135, CYS136, TYR139, ASN140, and ILE146
5F	-6.940	LEU92, LEU94, TYR97, TRP81, PRO82, PHE83, VAL87, MET132, ASN 135, CYS136, TYR139, ASN140, and ILE146

were 4E, 4A, 4B, 4F, 5D, 5F, and 3B (-8.499, -8.049, -7.620, -7.425, -7.361, -6.940 and -6.830 kcal mol^{-1}, respectively) ranked accordingly (Muvva *et al.*, 2014). The next 4 compounds were 5B, 3A, 4D, and 3C (-6.740, -6.685, -6.610, and -6.190 kcal mol^{-1}). The two least significant compounds were 4C and 4G (-5.741 and -4.267 kcal mol^{-1}). A higher glide docking score infers a better fit into BRD4's active site; more will be the ligand-protein interactions (Allen *et al.*, 2017).

The interaction between residues of bromodomain and extra terminal (BET) BRD4 protein (PDB ID-3MXF) with the experimental ligand compounds is shown in the ligand interaction diagrams (Fig. 1). These ligand interaction diagrams are for comparison between the standard ligand

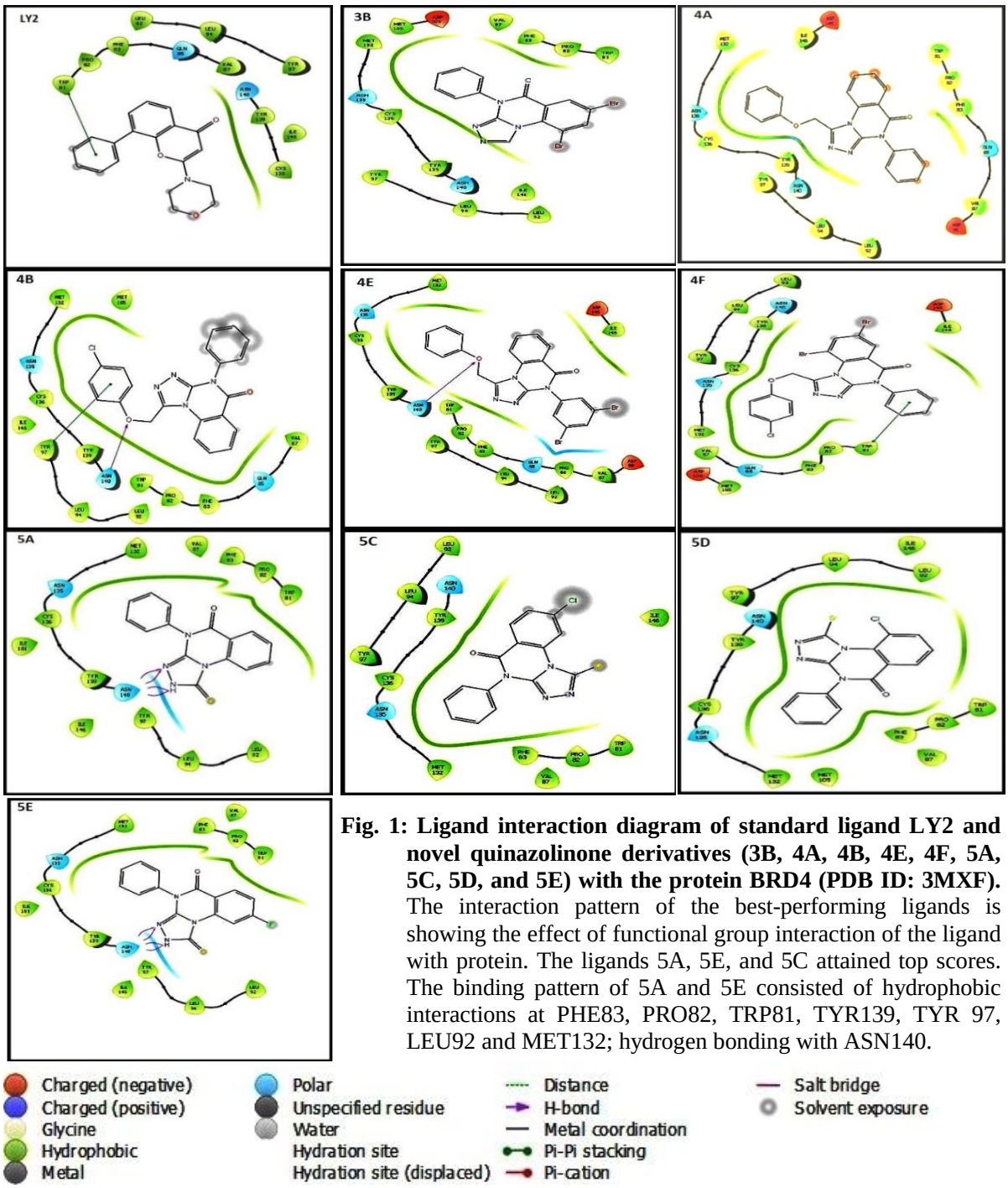

Fig. 1: Ligand interaction diagram of standard ligand LY2 and novel quinazolinone derivatives (3B, 4A, 4B, 4E, 4F, 5A, 5C, 5D, and 5E) with the protein BRD4 (PDB ID: 3MXF). The interaction pattern of the best-performing ligands is showing the effect of functional group interaction of the ligand with protein. The ligands 5A, 5E, and 5C attained top scores. The binding pattern of 5A and 5E consisted of hydrophobic interactions at PHE83, PRO82, TRP81, TYR139, TYR 97, LEU92 and MET132; hydrogen bonding with ASN140.

(LY2) and experimental ligands. These ligand interaction diagrams display a 2D diagram of interactions between the ligand and various amino acid residues of protein. Higher the matching pattern of experimental ligands with the standard ligand, better will be the ligand (Ferreira *et al.*, 2015). Fig. 1 shows the interactions of 12 amino acid residues of BRD4 protein (3MXF) with ligand LY2 (standard ligand). In LY2, the oxygen atom of ketonic group at 5^{th} position is mainly involved in H-bonding rest of the interactions are hydrophobic (Dhananjayan, 2015). The ligand interaction diagram showed that in BRD4-experimental ligand complexes, 12-17 amino acid residues were engaged in interactions with their respective experimental ligands. There were minimum of 10 and a maximum of 12 common interactions between ligand LY2 and experimental ligands, implying the quality interaction pattern similarity of ligands with LY2. Only 3A showed ten interactions, 3B, 4D, 4G, 5A, 5B, 5C, 5D, 5E, and 5F showed eleven interactions, and the remaining 3C, 4A, 4B, 4C, 4E, 4F showed all the 12 amino acid residues interaction of BRD4-LY2 complex Most common 10 interacting residues present in all experimental ligand complexes were LEU-92, LEU-94, TYR97, PRO82, PHE83, VAL87, CYS136, TYR139, ASN140, and ILE146. Most of the good scoring ligands interacted at ASN140, TYR97, MET132, and LYS91 with non-bonding interactions and hydrophobic interactions (Tahir *et al.*, 2018). The Glide dock score of all the compounds is given in Table 1, starting with standard ligand (LY2), followed by experimental ligands. The compounds with high binding affinity showed steric interactions at PRO82, PHE83, TYR97, MET132, MET105, and ASN135; and non-bonding interactions like hydrophobic interactions and steric interactions at ASN140, GLN85, TYR97, MET132, and LYS91 are also seen (Dhananjayan, 2015).

There are several quinazolinone based inhibitors that were synthesized and tested against cancerous proteins (Ajani *et al.*, 2016; Kavitha*et al*., 2018). These inhibitors showed a promising path in the direction of cancerous protein inhibition. There are very well-known drugs belonging to this class of inhibitors such a drug is LY2 (2-morpholin-4-yl-7-phenyl-4H-chromen-4-one) which we used as a benchmark against our experimental ligands. The docking experiment results were positive, and most of our ligands attained a higher glide score than LY2 (Table 1)**.**

Ligand 3A and derivatives

Quinazolinone and its derivatives have a very strong role in anticancer drug discovery (Singh *et al*., 2013). Our ligands have a basic quinazolinone structure and by addition of one ring and two nitrogen with one hydrogen to both nitrogen present at 3 and 1 position respectively we get our first derivative ligand 3A (Fig. 2). This ligand 3A produces 3B and 3C by addition of two bromine atoms at positions 3^{rd} and 5^{th} and two chlorine at 2^{nd} and 4^{th} position, respectively (Fig. 3). Ligand 3B have high score than 3A and 3C. In 3B, interacted with TRP81, VAL87, TYR139, and ILE146 through hydrophobic interactions. The bromine atom also contributes to the binding through halogen bonding.

Ligand 4A and derivatives

Ligand 4A (Fig. 4) has two rings, R1 and R2, and by the addition of hydrogen, chlorine, bromine, and a methyl group on these two rings, we get 7 more ligands 4A, 4B, 4C, 4D, 4E, 4F, 4G. In ligands 4A, 4B, 4C, and 4D, ring R1 remains unchanged, and modifications are only on the ring R2. The 4A has a single hydrogen attached to both the rings which gave the binding energy of -57.2873 kcal mol^{-1} and a glide docking score of -8.049 kcal mol^{-1} both are higher values that marks 4A as a highly capable ligand. In 4B, 4C, 4D ring R2 has the modifications of chlorine at position 4, a methyl group at position 2, and a methyl group at position 4, respectively. These modifications resulted in 4B with the score of -59.6333 kcal mol^{-1} of binding energy and glide docking score of -7.620 kcal mol^{-1}, followed by 4D with -53.3297 kcal mol^{-1} of binding energy and -6.610 kcal mol^{-1} of Glide docking score. Methyl group addition at position 2 of ring R2 in 4C has less significance as the Glide docking score is -5.741 kcal mol^{-1} with a binding energy of -52.9752 kcal mol^{-1}, although the binding energy score is among the leading ligand compounds.

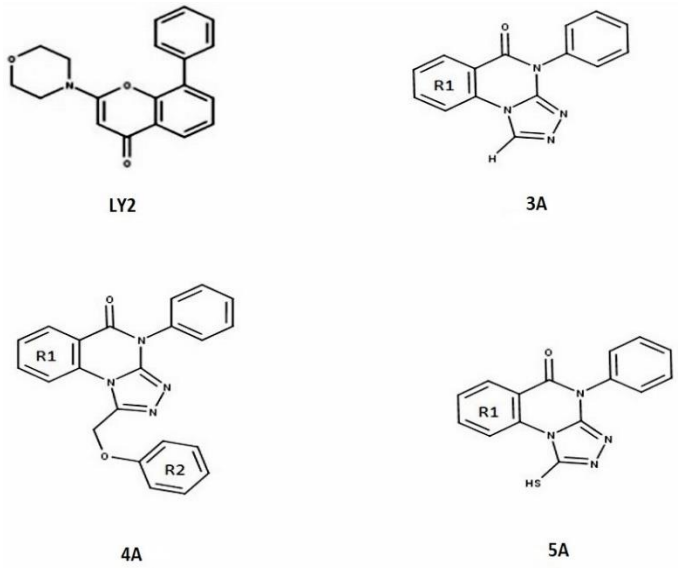

Fig. 2: Structure of LY2 (LY-294002, DrugBank ID: DB02656) (an established BRD4 inhibitor drug used as a standard ligand in this experiment). 3A, 4A and 5A (the three basic structures) of quinazolinone based derivatives. The ligand interaction diagrams of docked protein ligand complexes are very informative in analyzing the bonding pattern and interaction (Fig. 1).

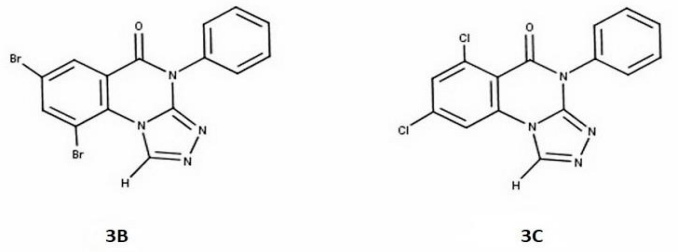

Fig. 3: Derivatives of Ligand 3A are 3B and 3C addition of bromine and chlorine on the ring R1of 3A created 3B and 3C, respectively.

Ligands 4E, 4F and 4G have both the rings R1 and R2 modified while R1 is changed with two bromine atoms at positions 3 and 5 in all the 3 ligands, R2 varies with the addition of hydrogen in 4E, giving binding energy of -60.5699 kcal mol^{-1} and higher Glide docking score of -8.499 kcal mol^{-1}, the oxygen of ligand 4E forms H-bond with ASN140, a key residue in better interacting ligands (Dhananjayan, 2015). A chlorine atom at position 4 in ring R2 also provides the best binding energy of -60.7798 kcal mol^{-1} with a Glide docking score of -7.425 kcal mol^{-1} in 4F. The addition of a methyl group at position 2 of ring R2 has a Glide docking score of -4.267 kcal mol^{-1} which is the lowest among all with binding energy -56.036 kcal mol^{-1} in 4G.

Ligand 5A and derivatives

5A had close structural similarity with ligand 3A, except it has sulphur with 5A we got 6 ligands 5A, 5B, 5C, 5D, 5E, and 5F. In 5A only hydrogen was added to the ring R1, 5B has two bromine atoms at 3rd and 5th positions, 5C has chlorine at 4th position, in 5D chlorine is at position 5th, 5E and 5F has fluorine and bromine at 4th position, respectively (Fig. 5). Ligand 5A has one ring R1 like that of 3A and the only change is of a hydrosulfide (HS) attachment. Ring R1 of 5A has a hydrogen atom with highest Glide docking score of -9.866 kcal mol^{-1} among all the experimental ligands and binding energy of -46.0075 kcal mol^{-1}, having two bromine atoms at 3 and 5 positions of R1, 5B scores -6.739 kcal mol^{-1} in Glide docking with the binding energy of -38.784 kcal mol^{-1} which is lowest among all experimental ligands. R1 of ligand 5C has chlorine at position 4 with a Glide dock score of -9.616 kcal mol^{-1} and the binding energy of the compound is -47.3005 kcal mol^{-1}. Chlorine at position 5 in R1 of 5D has a Glide dock score of -7.361 kcal mol^{-1} with a binding affinity of - 41.4502 kcal mol^{-1}. In 5E fluorine at position 4 of R1 improves the quality of ligand as it scores - 9.857 kcal mol^{-1} of Glide dock score with a binding energy of -45.7905 kcal mol^{-1}, the better performance of ligand 5A, 5E, and 5C is because of a conserved ASN140 residue of BRD4 protein that forms efficient hydrogen bonding with the ligand. TYR97 has also several hydrophobic interactions with the ligand (Jung *et al*., 2014). Bromine at position 4 of R1 in 5F scores -6.940 kcal mol^{-1} in docking and -40.3529 kcal mol^{-1} ranks the 5F as a mediocre ligand in all experimental ligand. The lower glide dock score has a basic reason that is, a lack of additional H bonding (Wang *et al.*, 2020) (Table 1).

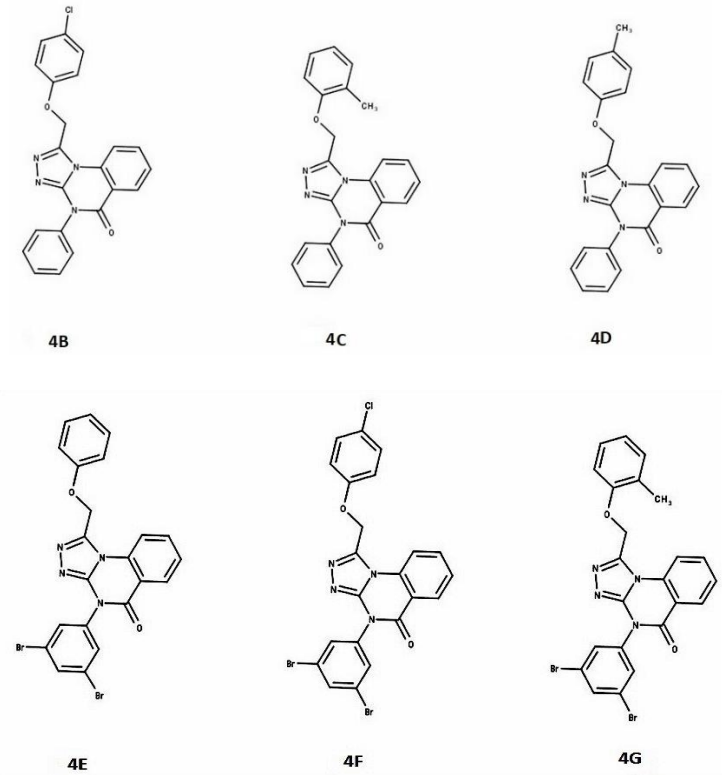

Fig. 4: Addition of chlorine and methyl group in ligand 4A generates 4B, 4C and 4D. 4B consists of a chlorine atom, 4C and 4D both have methyl group at different positions of ring R2 of ligand 4A. Ligand 4E have two bromine atoms at position 3 and 5 in ring R1. In ligands 4F and 4G Ring R1 remains same as of 4E, but ring R2 have a chlorine atom and a methyl group.

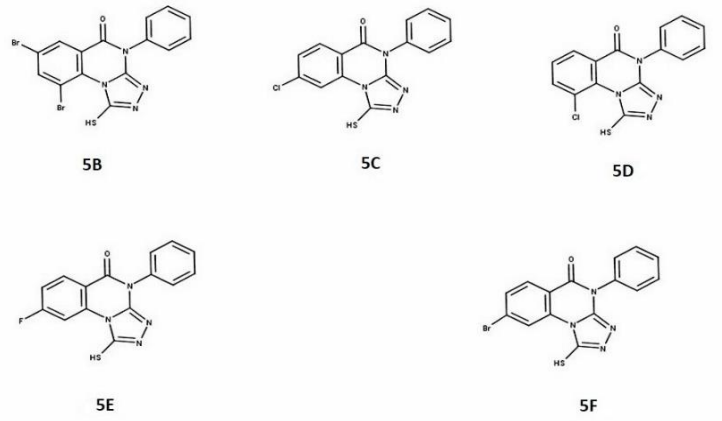

Fig. 5: Ligand 5A has different ring R1 in its derivatives 5B, 5C, 5D, 5E, and 5F. In 5B there are 2 bromine atoms, 5C and 5D both have a chlorine atom at different positions of ring R1. 5E has a fluorine atom, and 5F have a bromine atom at the same position of their R1 ring.

Aromatic rings of 5A, 5E and 5C are involved in the interactions with aromatic side chains of PHE83, TRP81, and TYR139. These bindings are significant. Halogen bonds are similar to hydrogen bonds in forming non-covalent and attractive interactions in protein-ligand complex and they also enhance the solubility and bioavailability of ligand-protein complexes. These factors make halogen bonding a novel tool in rational drug designing (Zhou *et al.*, 2010). In this work we used bromine, chlorine, and fluorine atoms in the experimental ligands and the results were impressive. This proved that the halogenation of ligand makes better drug candidates (Zhou *et al.*, 2010).

Binding energy calculation

The binding energy calculation was performed by using the prime MM-GBSA (Molecular Mechanics with Generalized Born and Surface Area solvation) module of Schrödinger 2017-2 (Jacobson *et al.*, 2004). In this method, docked pose file is needed as input, and the output is binding free energy of each ligand. These values are used to rank the compounds as per their binding affinity energy; higher negative values denote stronger binding affinity (Ferreira *et al.*, 2015). Ligand LY2 has a binding energy score of -51.2265 kcal mol^{-1}, and our experimental compounds had the values in between -38.784 and -60.7798 kcal mol^{-1}. The ligand 4F had highest binding energy followed by 4E, 4B, 4A, 4G, 4D, 4C, 3B, 5C, 5A, 5E, 3A, 5D, 3C, 5F, and 5B (-60.779, -60.569, -5.633, -57.287, -56.036, -53.329, -52.975, -50.691, -47.901, -46.007, -45.790, -45.405, -41.450, -40.392, -40.353, and -38.78 kcal mol^{-1}), respectively.

Table 2: Physiochemical properties of the lead compounds

Compounds	Molecular weight (g mol^{-1})	TPSA ($Å^2$)	HBA	HBD	Rotatable bond	MlogP	Water solubility
3B	420.06	52.12	3	0	1	4.75	Soluble
4A	368.39	61.42	4	0	4	4.09	Soluble
4B	390.82	61.42	4	0	4	4.09	Soluble
4E	526.16	61.42	4	0	4	4.59	Soluble
4F	560.16	61.42	4	0	4	5.94	Soluble
5A	294.33	90.99	3	0	1	3.48	Soluble
5C	328.78	90.99	3	0	1	4.00	Soluble
5D	328.78	90.99	3	0	1	4.00	Soluble
5E	312.32	90.99	4	0	1	3.88	Soluble

TPSA: Topology Polar Surface Area; HBA: Hydrogen bond acceptor; HBD: Hydrogen bond donor; MLogP: Partition coefficient

Ligands 5A, 5E, 5C, 4E and 4A are the top five ligands based on the Glide dock score. The consequence of the addition of one more parameter of binding energy for selection of the best ligand Ligands 5A, 5E, 5C, 4E and 4A are the top five ligands based on the Glide dock score. The consequence of the addition of one more parameter of binding energy for selection of the best ligand resulted in 4E with a Glide dock score of -8.499 kcal mol^{-1} and binding energy of -60.5699 kcal $mol^{-1,}$ but it is excluded because of the violation in drug-likeness (Table 3). In comparison with standard ligand LY2, the 10 experimental ligands out of 16 performed better, 4 ligands had marginally less glide dock score and 2 performed poorly. Ligand 5A, 5E, and 5C were the top scoring compounds and had slightly less binding energy than the standard ligand LY2. The drug-likeness filters of Lipinski, Ghose, Veber, Egan, and Muegge were also applied through the Swiss ADME server and the result showed the violation in compounds 3B, 4E and 4F (Table 3).

Drug-likeness analysis

ADME profiling provides quality assessment of lead compounds. The drug-likeness of top-scoring lead compounds were predicted (Table 2 and 3). Many compounds had a molecular weight of <500 g mol^{-1}. The hydrogen bond donor (HBD) and hydrogen bond acceptor (HBA) count were satisfactory for many lead compounds evaluated. MlogP values for many compounds were below 5 and all compounds were predicted as water-soluble. All compounds followed the Lipinski rule of five, except 3B, 4E and 4F. Compound 3B exceeded its MlogP value (>4.15), while 4E and 4F surpassed the limit of molecular weight (> 500 g mol^{-1}) and MlogP limit (>4.15). Ghose filter eliminated 4E and 4F due to molecular weight (> 480 g mol^{-1}). Another violation was of Muegge by compound 4F, rest compounds followed Lipinski, Ghose, Veber, Egan, and Muegge filter of drug-likeness. All the lead compounds passed the bioavailability score (> 0.10) so could be oral drug candidates (Daina *et al.*, 2017).

Table 3: Drug-likeness of lead compounds and bioavailability score

Compounds	Drug likeness					Bioavailability score
	Lipinski	Ghose	Veber	Egan	Muegge	
3B	No	Yes	Yes	Yes	Yes	0.55
4A	Yes	Yes	Yes	Yes	Yes	0.55
4B	Yes	Yes	Yes	Yes	Yes	0.55
4E	No	No	Yes	Yes	Yes	0.17
4F	No	No	Yes	Yes	No	0.17
5A	Yes	Yes	Yes	Yes	Yes	0.55
5C	Yes	Yes	Yes	Yes	Yes	0.55
5D	Yes	Yes	Yes	Yes	Yes	0.55
5E	Yes	Yes	Yes	Yes	Yes	0.55

Conclusion: The outcome of present study is encouraging as we have more competent ligands than our standard drug, LY2. We designed 16 novel compounds, of which 10 had a higher glide dock score than LY2, and only four scored marginally less than LY2. The screened compounds showed the potential of an anticancer drug candidate. The quinazolinone compounds and their derivatives again proved their anticancer drug-like properties and hold strong prospects against cancer. Drug designing is a complex and inventive process and *in silico* drug designing is a fundamental and effective way to start with. Synthesis and *in vitro* testing studies of these compounds will provide a much better conclusion regarding their use as an anticancer drug.

Conflict of interest: Authors declare that they have no conflict of interest.

Acknowledgment: Authors are very grateful to the Head, Department of Chemistry, Shibli National College for his kind guidance and support. Thanks are due to the Principal of the College for all the facilities provided.

REFERENCES

Ajani, O.O., Aderohunmu, D.V., Umeokoro, E.N. and Olomieja, A.O. 2016. Quinazoline pharmacophore in therapeutic medicine. *Bangladesh Journal of Pharmacology,* **11(**3): 716-733.

Allen, B.K., Mehta, S., Ember, S.W.J., Zhu, J.Y., Schönbrunn, E., Ayad, N.G. and Schürer, S.C. 2017. Identification of a novel class of BRD4 inhibitors by computational screening and binding simulations. *American Chemical Society (ACS) Omega*, **2**(8): 4760-4771.

Bray, F., Ferlay, J., Soerjomataram, I., Siegel, R.L., Torre, L.A. and Jemal, A. 2018. Global cancer statistics GLOBOCAN. *CA* (*A Cancer Journal for Clinicians),* **68**(6): 394-424.

Crisci, S., Amitrano, F., Saggese, M., Muto, T., Sarno, S., Mele, S., Vitale, P., Ronga, G., Berretta, M. and Di Francia, R. 2019. Overview of current targeted anti-cancer drugs for therapy in onco-hematology. *Medicina (Lithuania),* **55(**8): 1-28.

Daina, A., Michielin, O. and Zoete, V. 2017. SwissADME: A free web tool to evaluate pharmacokinetics, drug-likeness and medicinal chemistry friendliness of small molecules. *Scientific Reports,* **7**: 1-13.

Dhananjayan, K. 2015. Molecular docking study characterization of rare flavonoids at the Nac-binding site of the first bromodomain of BRD4 (BRD4 BD1). *Journal of Cancer Research,* **2015**:1-15. [*http://dx.doi.org/10.1155/2015/762716*].

Donati, B., Lorenzini, E. and Ciarrocchi, A. 2018. BRD4 and cancer: Going beyond transcriptional regulation. *Molecular Cancer,* **17**(1):1-13..

Ferreira, L.G., Dos Santos, R.N., Oliva, G. and Andricopulo, A.D. 2015. Molecular docking and structure-based drug design strategies. *Molecules,* **20**(7): 13384-13421.

Friesner, R.A., Murphy, R.B., Repasky, M.P., Frye, L.L., Greenwood, J.R., Halgren, T.A., Sanschagrin, P.C. and Mainz, D.T. 2006. Extra precision glide: Docking and scoring incorporating a model of hydrophobic enclosure for protein-ligand complexes. *Journal of Medicinal Chemistry*, **49**(21): 6177-6196.

Gerber, D.E. 2008. Targeted therapies: A new generation of cancer treatments. *American Family Physician,* **77**(3): 311-319.

Hanahan, D. and Weinberg, R.A. 2011. Review hallmarks of cancer : The next generation. *Cell,* **144**(5): 646-674.

Jacobson, M.P., Pincus, D.L., Rapp, C.S., Day, T.J.F., Honig, B., Shaw, D.E. and Friesner, R.A. 2004. A hierarchical approach to all-atom protein loop prediction. *Proteins: Structure, Function and Genetics,* **55(**2): 351-367.

Jung, M., Philpott, M., Müller, S., Schulze, J., Badock, V., Eberspächer, U., Moosmayer, D., Bader, B., Schmees, N., Fernández-Montalván, A. and Haendler, B. 2014. Affinity map of bromodomain protein 4 (BRD4) interactions with the histone H4 tail and the small molecule inhibitor JQ1. *Journal of Biological Chemistry*, **289**(13): 9304-9319.

Kavitha, K., Srinivasan, N. and Y, Haribabu. 2018. A review on quinazolinone and its derivatives with diverse biological activities. *World Journal of Pharmacy and Pharmaceutical Sciences*, **7**(4): 628-649.

Madhavi Sastry, G., Adzhigirey, M., Day, T., Annabhimoju, R. and Sherman, W. 2013. Protein and ligand preparation: Parameters, protocols, and influence on virtual screening enrichments. *Journal of Computer-Aided Molecular Design*, **27**(3): 221-234.

Muvva, C., Singam, E.R.A., Raman, S.S. and Subramanian, V. 2014. Structure-based virtual screening of novel, high-affinity BRD4 inhibitors. *Molecular BioSystems*, **10**(9): 2384-2397.

Nagaraju, G. 2015. Quinazoline: Unique and versatile pharmacophore in the filed of cancer. *Indo-American Journal of Pharmaceutical Sciences*, **2**(4): 827-832.

Padma, V.V. 2015. An overview of targeted cancer therapy. *Biomedicine*, **5**(4): 1-6.

Pucci, C., Martinelli, C. and Ciofani, G. 2019. Innovative approaches for cancer treatment: Current perspectives and new challenges. *Cancer Medical Science*, **13**: 1-26.

Saranath, D. and Khanna, A. 2014. Current status of cancer burden: Global and Indian scenario. *Biomedical Research Journal*, **1**(1): 1. [*https://doi.org/10.4103/2349-3666.240996*].

Singh, L.R., Kumar, M. and Shaharyar, M. 2013. Pharmacological evaluation of quinazolinone derivatives: A review. *Journal of Pharmaceutical and Bioanalytical Science*, **2**(3): 35-38.

Stathis, A., and Bertoni, F. 2018. BET proteins as targets for anticancer treatment. *Cancer Discovery*, **8**(1): 24-36.

Subramaniam, R., Rao, G. and Pai, S.P.N. 2011. 2D QSAR studies of some novel quinazolinone derivatives as antitubercular agents. *Journal of Computational Methods in Molecular Design*, **1**(3): 69-82.

Sung, H., Ferlay, J., Siegel, R.L., Laversanne, M., Soerjomataram, I., Jemal, A. and Bray, F. 2021. Global cancer statistics 2020: GLOBOCAN estimates of incidence and mortality worldwide for 36 cancers in 185 countries. *CA: A Cancer Journal for Clinicians*, **71**(3): 209-249.

Tahir, A., Alharthy, R.D., Naseem, S., Mahmood, N., Ahmed, M., Shahzad, K., Akhtar, M.N., Hameed, A., Sadiq, I., Nawaz, H. and Muddassar, M. 2018. Investigations of structural requirements for BRD4 inhibitors through ligand- and structure-based 3d qsar approaches. *Molecules*, **23**(7): 1-16.

Tiwary, B.K., Pradhan, K., Nanda, A.K. and Chakraborty, R. 2015. Implication of quinazoline-4(3H)-ones in medicinal chemistry : A brief review. *Journal of Chemical Biology and Therapeutics*, **1**(1): 1-7.

Wang, L., Xu, M., Kao, C.Y., Tsai, S.Y. and Tsai, M.J. 2020. Small molecule JQ1 promotes prostate cancer invasion via BET-independent inactivation of FOXA1. *Journal of Clinical Investigation*, **130**(4): 1782-1792.

Weinstein, I.B. and Joe, A. 2008. Oncogene addiction. *Cancer Research*, **68**(9): 3077-3080.

White, M.E., Fenger, J.M. and Carson, W.E. 2019. Emerging roles of and therapeutic strategies targeting BRD4 in cancer. *Cellular Immunology*, **337**: 48-53.

Xu, Y. and Vakoc, C.R. 2017. Targeting cancer cells with BET bromodomain inhibitors. *Cold Spring Harbor Perspectives in Medicine*, **7**(7): 1-17.

Zhou, P., Tian, F., Zou, J. and Shang, Z. 2010. Rediscovery of halogen bonds in protein-ligand complexes. *Mini-Reviews in Medicinal Chemistry*, **10**(4): 309-314.